Neural Computing and Applications (2020) 32:15857–15868
https://doi.org/10.1007/s00521-018-3889-z

RECENT ADVANCES IN DEEP LEARNING FOR MEDICAL IMAGE PROCESSING

A deep convolutional neural network model for automated identification of abnormal EEG signals

Özal Yıldırım[1] · Ulas Baran Baloglu[1] · U. Rajendra Acharya[2,3,4]

Received: 17 September 2018 / Accepted: 12 November 2018 / Published online: 23 November 2018

Abstract
Electroencephalogram (EEG) is widely used to monitor the brain activities. The manual examination of these signals by experts is strenuous and time consuming. Hence, machine learning techniques can be used to improve the accuracy of detection. Nowadays, deep learning methodologies have been used in medical field to diagnose the health conditions precisely and aid the clinicians. In this study, a new deep one-dimensional convolutional neural network (1D CNN) model is proposed for the automatic recognition of normal and abnormal EEG signals. The proposed model is a complete end-to-end structure which classifies the EEG signals without requiring any feature extraction. In this study, we have used the EEG signals from temporal to occipital (T5–O1) single channel obtained from Temple University Hospital EEG Abnormal Corpus (v2.0.0) EEG dataset to develop the 1D CNN model. Our developed model has yielded the classification error rate of 20.66% in classifying the normal and abnormal EEG signals.

Keywords Convolutional neural network · Abnormal EEG · EEG classification · Deep learning

1 Introduction

Electroencephalogram (EEG), which monitors the electrical brain activity, is a valuable and cost-effective tool used to detect many neurological disorders [1–11]. The major diseases identified and monitored using EEG signals are epilepsy [1–3], seizure [4, 5], Alzheimer [6–8], Parkinson's disease [9], depression [10], and sleep disorders [11]. Brain waves are produced by mounting a certain number of electrodes on the scalp (i.e., 10–20 systems) according to the standard sets [12, 13]. Recent advances in the technology have made it easier to collect and store these signals. However, human professionals are still required to evaluate the EEG signals. Neurologists usually evaluate these signals by visual inspection, which is time consuming [4]. Therefore, the development of fully automated solutions is very crucial in this research field.

The EEG signals can be classified according to their frequency, amplitude, and amplitude on the scalp [14]. During the classification, first the class (normal or abnormal) of the given signal needs to be determined. Subsequently, the type of neurological disorder can be analyzed by dividing the abnormal signals into sub-categories. In the abnormal EEG signals, the electrical activities between neurons occur in an abnormal fashion, and these states are called as seizures. If this abnormality spreads to all regions of the brain, it is classified as a generalized seizure. If the seizure occurs only in specific regions, then it is classified as a focal or partial seizure [15, 16]. During the acquisition of EEG signals, bioelectrical artifacts have to be carefully eliminated by analyzing the seizures with several montages to avoid external and false interpretations [17]. The correct classification of seizures as epileptic and non-epileptic helps in the diagnosis of major illnesses such as epilepsy [2]. Seizures do not always occur, and typical EEG signals are called normal when they do not contain any unusual seizures [14]. Since seizure detection is the preliminary

✉ Özal Yıldırım
oyildirim@munzur.edu.tr; yildirimozal@hotmail.com

[1] Department of Computer Engineering, Engineering Faculty, Munzur University, 62100 Tunceli, Turkey

[2] Department of Electronics and Computer Engineering, Ngee Ann Polytechnic, Singapore, Singapore

[3] Department of Biomedical Engineering, School of Science and Technology, Singapore School of Social Sciences, Singapore, Singapore

[4] Faculty of Health and Medical Sciences, School of Medicine, Taylor's University, 47500 Subang Jaya, Malaysia

stage for the detection of abnormal brain functions, many studies in the literature are focused on the detection [4, 5, 18, 19] and prediction [20–24] of seizure.

The most common sequential steps involved in the development of the automated diagnosis system are preprocessing, feature extraction, and classification [25, 26]. In the preprocessing stage, normalization and various transformations are applied to the raw signals to standardize the model for the successive stages. In the feature extraction stage, the distinctive signatures present in the signals are extracted using various methods. The commonly used feature extractors are wavelet transform [3, 27–30], Hilbert–Huang transform [31], higher-order cumulant and spectra features [32, 33], and component analysis [8, 34, 35]. The classifiers such as neural network [36] and support vector machines [16, 32, 33] are widely used for the classification of features obtained by handcrafted feature extraction methods. Single-channel or multi-channel signals are used to perform the analysis [37].

The complex and nonlinear nature of EEG signals require the development of more innovative machine learning and signal processing methods for their analysis [8, 9]. Recent advances in the field of deep learning methodologies have resulted in promising approaches for automatic extraction of complex data features at high levels of abstraction [38–40]. Recently, these deep learning algorithms have been successfully employed in image processing [41–44], natural language processing [45], speech processing [46], and computer games [47]. These algorithms also have been used in the biomedical field [22, 48–51]. Acharya et al. [4] proposed a 13-layer deep convolutional neural network (CNN) for the classification of normal, pre-ictal, and seizure EEG signals. In this study, they reported a classification rate of 88.67% using 300 EEG signals from five patients. The same group [10] proposed a novel EEG-based depression screening system using a deep neural network approach. In this study, 93.5% (left hemisphere) and 96.0% (right hemisphere) success rates are reported using 15 normal and 15 depressed patients. In another study, Oh et al. [9] proposed a deep learning approach for the diagnosis of Parkinson's disease using EEG signals. They achieved an accuracy of 88.25% with 13-layer CNN model developed using 20 healthy and 20 Parkinson's disease subjects.

In this study, a deep learning-based approach is proposed for the automated recognition of normal and abnormal EEG signals. A 23-layer complete end-to-end 1D-CNN-based model is presented instead of the manual feature extraction method. Abnormal EEG signals are automatically recognized from 1-min sections of the EEG recordings. This recognition process is performed on single-channel input data obtained from Temple University Hospital (TUH) dataset. The goals of the work are: abnormal EEG detection for the diagnosis of neurological disorders and application of deep learning technique for the neuroscience using big EEG database. The motivation is fact, that manual examination of EEG signals by experts is strenuous and time consuming, and therefore, machine learning methods can improve the accuracy of detection. For this purpose, a new 1D CNN model was constructed and employed for the first time on the TUH EEG corpus sub-database to achieve these goals. Another notable achievement was the successful usage of only single-channel 1-min EEG segments instead of multi-channel derived segments. Furthermore, in this study the identification task does not require a brain scan which is beneficial for medical diagnosis.

The rest of this paper is organized as follows. Section 2 introduces the materials, methods and the proposed 1D CNN model. The experimental setup and the obtained performance of the proposed model are given in Sect. 3. Section 4 provides the discussion based on the results obtained in Sect. 3. Finally, the paper concludes in Sect. 5.

2 Materials and methods

In this study, a deep convolutional neural network model was used for the classification of normal and abnormal EEG signals. This model allows the signals to be entirely recognized through an end-to-end complete structure without any feature extraction stage. The EEG dataset used in the study was recorded at the Temple University Hospital. Figure 1 shows the block diagram showing the steps involved in the automated recognition of abnormal EEG signals.

2.1 EEG dataset description

The TUH EEG Corpus database [52] is the world's largest publicly accessible EEG database, comprising over 28,000 EEG records collected since 2002. The purpose of creating these data sets is to supply enough clinical data for the development of data-oriented tools and provide an infrastructure for the progress of research. The most powerful feature of this database is having a report provided by the clinician for each EEG signal. These reports include the patient's clinical history and summary of the medication. In this study, we have used TUH abnormal EEG Corpus (v2.0.0) dataset which consists of normal and abnormal EEG signals. These signals are presented in two groups as training and evaluation. Table 1 provides the distribution of patients and sessions employed in TUH EEG Abnormal Corpus (v2.0.0) dataset.

There is no conflict in the patients during the training and evaluation datasets. In the evaluation dataset, only one

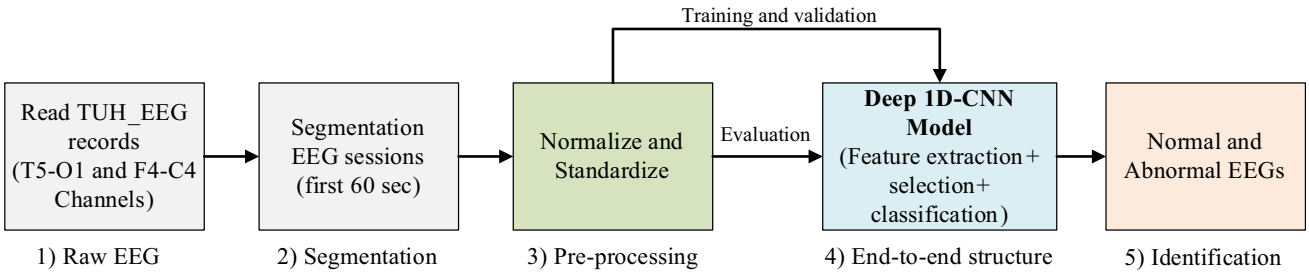

Fig. 1 Steps involved in the automated detection of abnormal EEG signals

Table 1 Distributions of patients and sessions employed in TUH EEG Abnormal Corpus (v2.0.0)

Description	Patients			Sessions		
	Normal	Abnormal	Total	Normal	Abnormal	Total
Train	1237	893	2130	1371	1346	2717
Evaluation	148	105	253	150	126	276
Total	1385	998	2383	1521	1472	2993

patient record either normal or abnormal is used. Few patient records exist more than once during the training. As a result, there are 253 unique patients in the evaluation of dataset and 2076 unique patients in the training dataset. There can be more than one session per patient. The distribution of the patients in the EEG database is shown in Table 2.

The records in the EEG database have signals from 24 to 36 channels, and channels are annotated which contains interesting event markers. The EEG signals were obtained with a sampling frequency of 250 Hz with 16 bits per sample. The left side of Fig. 2 shows the channel sensor locations used to obtain the records and the right side provides the first 60-s signal samples of an abnormal record. A typical EEG system has a montage of 19 electrodes, but more electrodes can be used to increase the collected spatial data.

2.2 Proposed 1D Convolutional Neural Network Model

A new 1D convolutional neural network model is designed for the automated classification of normal and abnormal EEGs. The designed deep network model has 23 layers including the input layer. The developed model has 1D Convolution (Conv), MaxPooling (MaxP), dropout, batch normalization, and dense layers. Figure 3 shows the proposed deep 1D CNN model.

Table 2 Gender distribution of patients in the EEG data set

Description	Train		Evaluation	
	Patients	Files	Patients	Files
Normal (female)	691	768	84	85
Normal (male)	546	603	64	65
Abnormal (female)	454	679	51	63
Abnormal (male)	439	667	54	63
Total	2130	2717	253	276

The first layer of the model consists of raw EEG signals. The convolution layer, which comes after the input layer, performs the convolution operation on the input signal with *three* stride intervals and *eight* filters with 23 elements. After the convolution process, feature maps of the input signal are created. In the MaxP layer, two-unit regions on these feature maps are reduced to the maximum value in these regions. Thus, the size of the input feature map is reduced by half, depending on the pooling size and stride values. One of the biggest challenges in deep architecture is overfitting. The most common technique used to prevent overfitting is dropout [53]. In the proposed deep model, dropout layers are added in various positions to protect it from the overfitting. The batch normalization layers are used in the model to normalize the activations of the previous layer in each batch. During batch normalization, the model maintains a near-zero activation average and a near-one activation standard deviation with the conversion method. The dense layers have the deeply connected neural network structure. Dimension transformations are performed in the flattened layer so that the properties in the previous layers can be processed in dense layers. The last layer of the model is the softmax layer which performs the classification process. In this layer, input EEG data are classified as normal or abnormal. The details and the employed parameters of the proposed 1D CNN model are given in Table 3.

The total number of parameters of the model is 382,682 of which 382,634 are trainable, and 48 are non-trainable

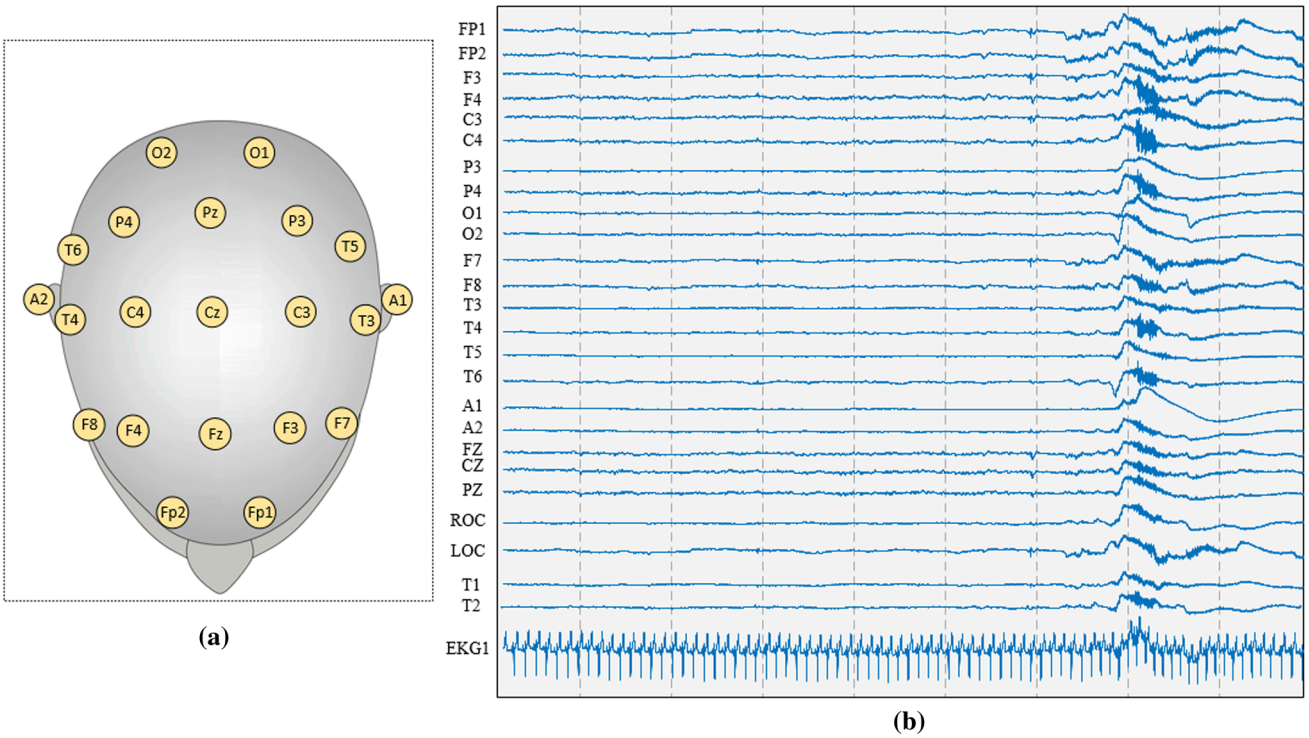

Fig. 2 Electrode locations and channel samples used during the acquisition of EEG records: **a** visual representation of the placements of the EEG sensors, **b** first 60 s EEG signals from channels of an abnormal record in the TUH EEG corpus database

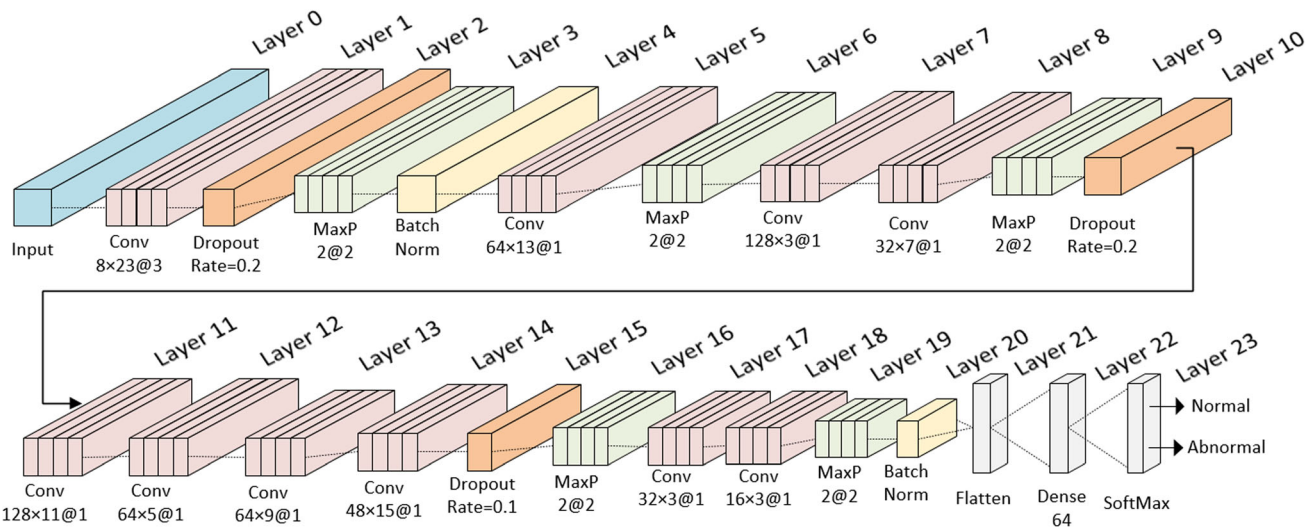

Fig. 3 Block representation of the proposed deep 1D CNN model

parameters. Kernel size parameter represents the 1D convolution window size. Overfitting is the biggest problem during the design stage of the model. The optimum model is determined after numerous adjustments in the number of layers and hyper-parameters. The brute force technique is used to determine the number of layers of the 1D CNN model and parameters of these layers. During validation, the optimum layers and parameter adjustments are made by continuously to obtain the best results.

3 Experimental results

In this section, the experimental results obtained using the proposed CNN model to detect the abnormal EEG signal are presented. The details and specifications of the experimental environment are given. Then the results of the proposed recognition system are presented and discussed.

Table 3 Detailed information about the layers and parameters used in the proposed 1D CNN model

No.	Layer name	Kernel size	Layer parameters	Number of parameters	Output shape
0	Input	–	–	–	15,000 × 1
1	Conv1D	8 × 23	Stride = 3, Activation = ReLU	376	4993 × 8
2	Dropout	–	Rate = 0.2	0	4993 × 8
3	MaxP	2	Stride = 2	0	2496 × 8
4	Batch Norm.	–	–	32	2496 × 8
5	Conv1D	64 × 13	Stride = 1, Activation = ReLU	6720	2484 × 64
6	MaxP	2	Stride = 2	0	1242 × 64
7	Conv1D	128 × 3	Stride = 1, Activation = ReLU	24,704	1240 × 128
8	Conv1D	32 × 7	Stride = 1, Activation = ReLU	28,704	1234 × 32
9	MaxP	2	Stride = 2	0	617 × 32
10	Dropout	–	Rate = 0.2	0	617 × 32
11	Conv1D	128 × 11	Stride = 1, Activation = ReLU	45,184	607 × 128
12	Conv1D	64 × 5	Stride = 1, Activation = ReLU	41,024	603 × 64
13	Conv1D	64 × 9	Stride = 1, Activation = ReLU	36,928	595 × 64
14	Conv1D	48 × 15	Stride = 1, Activation = ReLU	46,128	581 × 48
15	Dropout	–	Rate = 0.1	0	581 × 48
16	MaxP	2	Stride = 2	0	290 × 48
17	Conv1D	32 × 3	Stride = 1, Activation = ReLU	4640	288 × 32
18	Conv1D	16 × 3	Stride = 1, Activation = ReLU	1552	286 × 16
19	MaxP	2	Stride = 2	0	143 × 16
20	Batch Norm.	–	–	64	143 × 16
21	Flatten	–	–	0	2288
22	Dense	64	Activation = ReLU, Dropout = 0.1	146,496	64
23	Softmax	2	Activation = Softmax	130	2

3.1 Experimental setup

For automatic recognition of normal and abnormal EEG signals, abnormal EEG corpus dataset TUH EEG database was used. The records of this database are presented in two parts as training and evaluation. During the experimental studies, these data are used for training and testing the model. The experimental setup of this study was proposed by Lopez et al. [54] who preferred to use first 60-s samples of EEG records. The EEG records in the database contain the signals gathered from 24 to 36 different channels. Only posterior temporal to occipital (T5–O1) and right frontal to central (F4–C4) channel signals were used in both [54] and this study. The most promising channel which can be used for manual interpretation is the T5–O1 differential measurement which is part of the popular Temporal Central Parasagittal (TCP) montage [55]. The F4–C4 channel signal was examined for comparison purpose. Figure 4 represents the visual representation of T5–O1 and F4–C4 EEG signals in the TCP assembly.

In this study, the first 60-s sections of each EEG record were used. Each of these segments comprises of 15,000 samples and were fed as input to the CNN model. No handcrafted feature extraction has been performed on the signals. At the preprocessing stage, the signals are normalized to 0–1, and then the signals were standardized by removing the mean and scaling to unit variance. Figure 5 shows the first 60-s sections of normal and abnormal EEG records of T5–O1 channel EEG signal.

Our deep learning architecture model was developed using Keras whose libraries are written in Python [56]. The entire experimental was carried out on a computer with Intel Core i7-7700HQ 2.81 GHz CPU, 16 GB RAM and NVIDIA GeForce GTX 1070 8 GB graphics card. The main hyper-parameters used during the execution of CNN architecture are given in Table 4.

3.2 Results

In this study, a deep learning model was developed for the automatic classification of normal and abnormal EEG signals. The EEG signals from TUH EEG database were used. The EEG database records are split into two parts: training and evaluation. The train dataset was used during

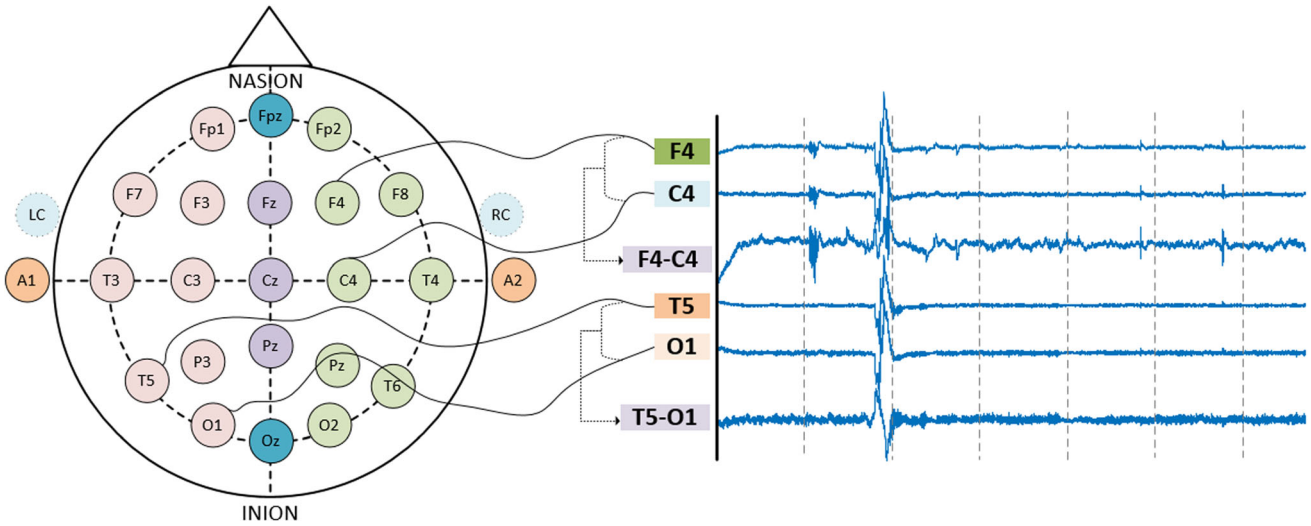

Fig. 4 Graphical representation of the acquisition of T5–O1 and F4–C4 EEG signals in the TCP assembly

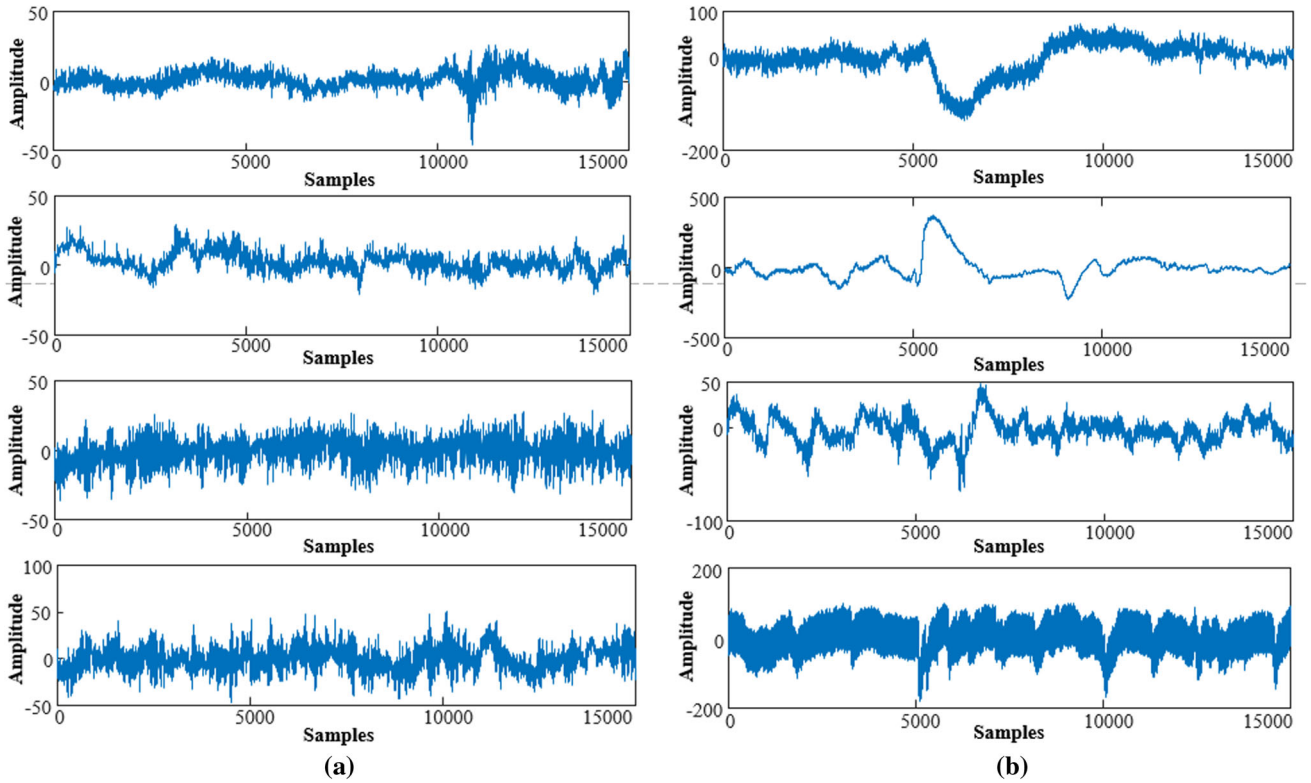

Fig. 5 Waveforms of first 60 s sections of T5–O1 channel EEG signals: **a** normal EEG samples, **b** abnormal EEG samples

the learning stage, and evaluation data was used during the testing stage. 80% of the training data are used to train the CNN model, and remaining 20% are used as the validation data. Thus, 2173 out of a total of 2717 records were used for training, and the remaining 544 were used for the validation. The distributions of these data were randomly selected. Different data sets are used for validation purpose since the parameter setting operations of the model consists of many stages. However, experimental results are obtained with a particular random seed value to ensure the reproducibility and consistency of the model. A detailed illustration of the data used for this work is shown in Fig. 6.

Experimental results are obtained for T5–O1 channel which is usually considered by the experts. The

Table 4 Hyper-parameter values of the proposed deep CNN model

No.	Parameters	Values
1	Optimizer	Adam, beta1 = 0.9 and beta2 = 0.999
2	Learning rate	0.00001
3	Decay	1e−3
4	Loss function	Categorical cross entropy
5	Metrics	Accuracy
6	Batch size	128
7	Epoch	150

performance graphs of the CNN model during the training phase for 150 epochs for this channel are given in Fig. 7.

It can be seen from the performance graphs that, there is no overfitting problem in the model. During the training phase of the model, the training accuracy is in the range of 78–79% and validation accuracy rate is found to be 79–80%. The train loss value, which started at 0.78, decreased to 0.46. The model could not finish the training phase successfully because of the challenging data. Experiments carried out with different hyper-parameters have observed overfluctuations and overfitting problems during the train and validation, even after the model complete training phase.

Another critical performance achievement of the trained CNN model is its success with the test data that it is never met during the training phase. For this purpose, various evaluation criteria have been selected for the test data. These criteria are accuracy, precision, recall, and F1-Score. A brief description of these criteria and related equations are given below. The abbreviations used in these calculations are true positive (TP), false positive (FP), true negative (TN), and false negative (FN).

- *Accuracy* It is a ratio of correctly estimated observations to total observations. It is a widely used evaluation criterion, and its calculation is shown in Eq. (1).

$$\mathrm{Acc}(\%) = \frac{\mathrm{TP} + \mathrm{TN}}{\mathrm{TP} + \mathrm{FP} + \mathrm{FN} + \mathrm{TN}} \times 100 \quad (1)$$

- *Precision* It is the ratio of correctly estimated positive observations to total estimated positive observations. It can be evaluated by Eq. (2).

$$\mathrm{Precision}(\%) = \frac{E}{\mathrm{TP} + \mathrm{FP}} \times 100 \quad (2)$$

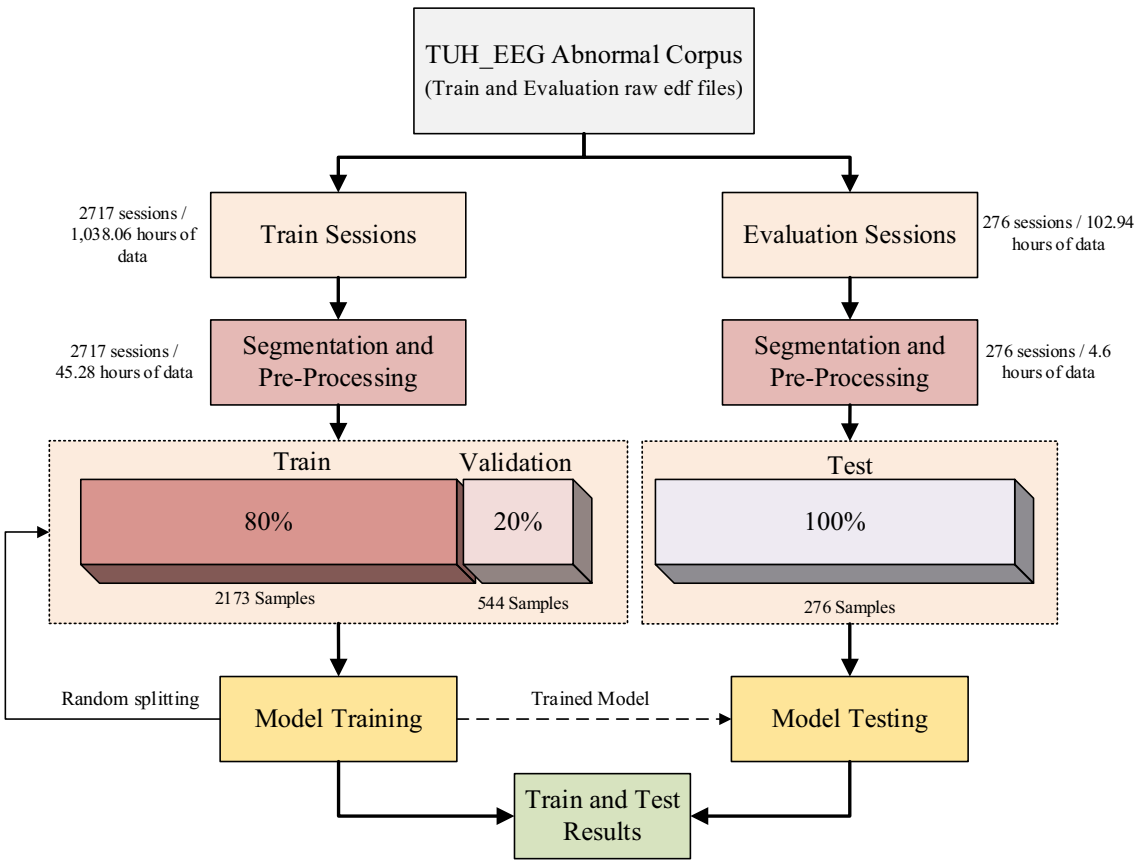

Fig. 6 The illustration of data used to develop the proposed model

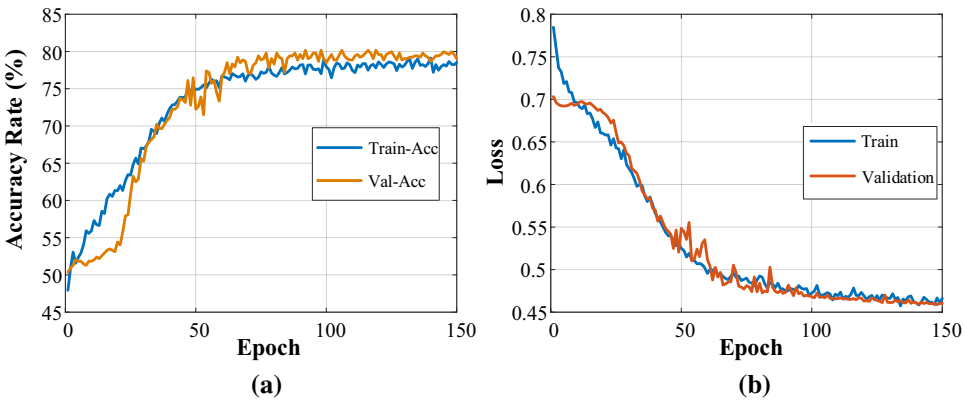

Fig. 7 Performance graphs of the model during the training phase with T5–O1 channel EEG signals: **a** model accuracy, **b** model loss

- *Recall* It is the ratio of correctly classified observations in a class to all observations in that class. Recall is also commonly known as sensitivity. It is given by Eq. (3).

$$\text{Recall}(\%) = \frac{\text{TP}}{\text{TP} + \text{FN}} \times 100 \tag{3}$$

- *F1-Score* It is the weighted average of precision and recall values. It can be calculated by Eq. (4).

$$\text{F1} - \text{Score} = \frac{(\text{recall}) \times (\text{precision}) \times 2}{(\text{recall}) + (\text{precision})} \tag{4}$$

The developed model trained using T5–O1 signal is evaluated with 276 sessions. Table 5 presents the various performance measures obtained for the developed model.

Our developed CNN model classified the test EEG signals with an average precision ratio of 79.64% and recall rate of 78.91%. The confusion matrix obtained for the model for the test data is given in Table 6.

The proposed model correctly classifies 219 of 276 T5–O1 EEG signals, resulting in an accuracy of 79.34%. 21 out of 150 regular EEG signals are identified incorrectly, and 36 of 126 abnormal EEG signals are wrongly classified. Thus, we have obtained an error rate of 20.66% using T5–O1 channel EEG signals.

We have evaluated the performance of the model using F4–C4 channel EEG signal without changing any model parameters. Figure 8 shows the performance graphs of the developed model using F4–C4 channel EEG signals during 150 epochs of the training stage.

Table 6 Confusion matrix obtained for the developed model using T5–O1 channel EEG data

Class	Normal EEG	Abnormal EEG
Normal EEG	TP = 129 (86%)	FN = 21 (14%)
Abnormal EEG	FP = 36 (28.57%)	TN = 90 (71.42%)
Overall accuracy = 79.34%		

For the model trained using F4–C4 channel EEG data, the overfitting problem did not occur during the training phase, and the validation accuracy rate of 73–74% is obtained. The loss value, which was 0.70 during the training of the model, decreased to 0.51 at the end of 150 epochs. The model trained with F4–C4 EEG channel data was fed with 276 test data. Table 7 presents the various performance measures obtained for the developed model.

Our developed CNN model classified the test EEG signals from F4 to C4 channel with an average precision ratio of 77.08% and recall rate of 73.1%. The confusion matrix obtained for the model for the test data is given in Table 8.

The proposed model correctly classified 136 of 150 F4–C4 channel EEG signals, resulting in an accuracy of 74.63%. The model showed slightly lower performance in recognizing the abnormal EEG signals.

Our results show that the developed model performed better using T5–O1 channel EEG data than using F4–C4 channel EEG data both during training and testing stages.

Table 5 Performance measures of the proposed model using T5–O1 channel test data

Class	Precision ratio (%)	Recall ratio (%)	F1-Score (%)	Accuracy rate (%)	Number of data
Normal EEGs	78.18	86.00	81.90	79.34	150
Abnormal EEGs	81.11	71.42	75.95		126
Avg/total	79.64	78.71	78.92		276

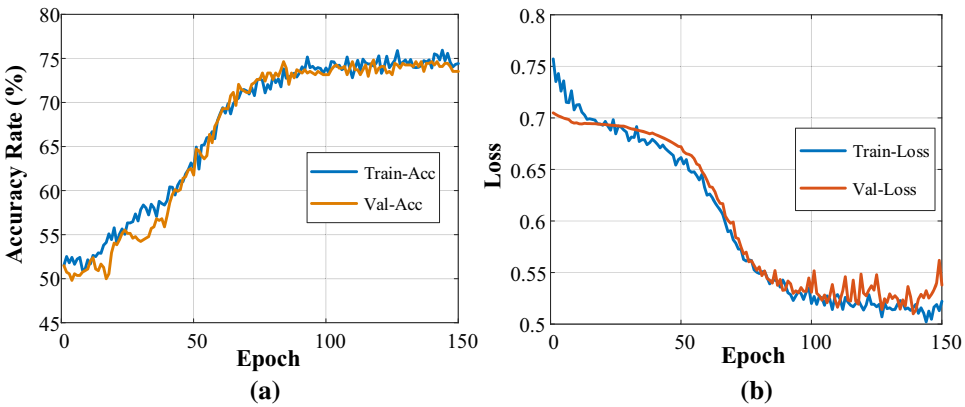

Fig. 8 Performance graphs of the model during the training phase with F4–C4 channel EEG signals: **a** model accuracy, **b** model loss

Table 7 Performance measures of the proposed model using F4–C4 channel test data

Class	Precision ratio (%)	Recall ratio (%)	F1-Score (%)	Accuracy rate (%)	Number of data
Normal EEGs	70.83	90.66	79.52	74.63	150
Abnormal EEGs	83.33	55.55	66.66		126
Avg/total	77.08	73.10	73.09		276

Table 8 Confusion matrix obtained for the developed model using F4–C4 channel EEG data

Class	Normal EEG	Abnormal EEG
Normal EEG	TP = 136 (90.66%)	FN = 14 (9.33%)
Abnormal EEG	FP = 56 (44.44%)	TN = 70 (55.55%)
Overall accuracy = 74.63%		

The hyper-parameters of the model were not changed for both channel EEG signals. Figure 9 shows the comparative graphs of the performances of the developed model using T5–O1 and F4–C4 channels EEG signals during the training stage.

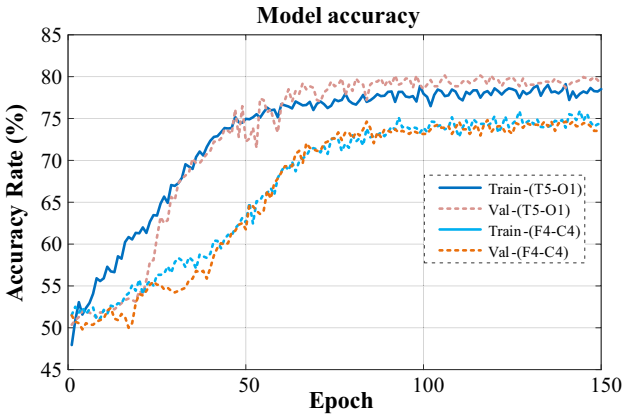

Fig. 9 Performance graphs of the developed model during training level using T5–O1 and F4–C4 channel EEG signals

4 Discussion

In this study, TUH EEG abnormal dataset is used to classify normal and abnormal EEGs using 1D CNN model. Table 9 presents the summary of results obtained for automated detection of abnormal EEG signal using TUH EEG abnormal corpus dataset.

The experimental setup used for this data collection is provided in Lopez et al. [54]. They performed feature extraction using 0.1 s frame duration for the first 60 s frames of T5–O1 channel signals in their study. They reduced the size of feature vectors using the class-dependent principal component analysis (PCA) method, and classified the obtained feature vectors using k-Nearest neighbor (kNN) and Random forest (RF) classifier. The proposed approach classified the EEG data with an error rate of 41.8% with kNN and 31.7% with RF classifier. Lopez [57] used four-channel EEG signals for a 7-s frame duration of the first 60-s frame for the detection of abnormal EEG signals. They reported an error rate of 21.2% for the occipital region with 2D CNN model.

In this study, only normalization and standardization preliminary operations are performed on the EEG signals. The first 60-s (15,000 samples) segments of the T5–O1 channel EEG records are used in this study. The developed 1D CNN model automatically recognizes normal and abnormal records with an error rate of 20.6%. Other than

Table 9 Performance comparison of the proposed recognition system with other works reported using the same dataset

Study	Method	Number of used channels	Input size (s)	Error rate (%)	Dataset
Lopez et al. [54]	kNN (k = 20)	One channel	0.1	41.8	Abnormal (v1.x.x)
	RF (N_t = 50)	One channel	0.1	31.7	Abnormal (v1.x.x)
Lopez [57]	2D CNN + MLP	Four channel	7	21.2	Abnormal (v1.x.x)
Proposed study	1D CNN	One channel	60	20.6	Abnormal (v2.0.0)

automatic feature extraction, 1D CNN model has further advantages such as extraction of 1D subsequences from the signal with reduced number of features and processing within the convolution layer. These advantages make 1D CNN model is suitable for the single-channel EEG signal structure.

In [54], PCA coupled with classifiers (KNN and RF) are used for the detection of abnormal EEG signals using 0.1 s frame duration T5–O1 channel signals. In another study by the same group used four-channel EEG signals and used 7-s frame duration [57]. In this work, we have used single-channel EEG signal for 60 s duration. Table 9 shows that with the increase in the frame duration, the error rate decreases (accuracy increases). This is because, with the increase in the length of the signal, more subtle information can be extracted from the time series. Hence, the classification accuracy increases.

The significant contributions of this study are as follows:

- The application of 1D CNN deep learning approach on the largest EEG database TUH EEG.
- The first 1D CNN study on the TUH EEG Abnormal Corpus (v2.0.0) sub-database.
- Automated identification of abnormal signals using 1-min EEG segments.
- EEG-based abnormality identification without a brain scan.
- Diagnosis is based on only single-channel EEG with high accuracy (error rate is 20.6%)

The major drawbacks of this study are as follows:

- The developed model is huge having 23 layers.
- Only the first 1-min segments are used for each record.

In this study, an experiment is conducted using new version of the TUH EEG abnormal dataset without changing the existing experimental setup. In future studies, we intend to use lengthy duration data for the analysis. Also, we propose to perform classification using multiple channel EEG signals of brain. In this study, only the first 60-s sections of each EEG records are used as input data. The number of data records can be increased by reducing the segment durations. Apart from the CNN algorithm, other deep learning algorithms such as LSTM, CNN + LSTM can be implemented to improve the classification accuracy.

5 Conclusion

It is very challenging to detect the brain abnormalities using EEG signals. The accurate detection of abnormal EEG signals can help to provide proper treatment to the patients early and hence improve the quality of life. In this study, we have proposed a 1D-CNN-based approach for the automated detection of abnormal EEG signals. Our developed system is able to detect the abnormal EEG signals with an accuracy of 79.34%, precision rate of 79.64%, and sensitivity of 78.71%. This developed system can aid the clinicians to validate their screening of EEG signals. In the future, we intend to improve the performance of this work by cascading this model with other deep learning models like Long Short-Term Memory (LSTM).

Compliance with ethical standards

Conflict of interest There is no conflict of interest in this work.

References

1. Smith SJM (2005) EEG in the diagnosisclassification, and management of patients with epilepsy. J Neurol Neurosurg Psychiatry. https://doi.org/10.1136/jnnp.2005.069245
2. Acharya UR, Vinitha Sree S, Swapna G et al (2013) Automated EEG analysis of epilepsy: a review. Knowl Based Syst 45:147–165
3. Işik H, Sezer E (2012) Diagnosis of epilepsy from electroencephalography signals using multilayer perceptron and Elman artificial neural networks and wavelet transform. J Med Syst 36:1–13
4. Acharya UR, Oh SL, Hagiwara Y et al (2018) Deep convolutional neural network for the automated detection and diagnosis of seizure using EEG signals. Comput Biol Med 100:270–278
5. Chen G (2014) Automatic EEG seizure detection using dual-tree complex wavelet-Fourier features. Expert Syst Appl 41(5):2391–2394

6. Lehmann C, Koenig T, Jelic V et al (2007) Application and comparison of classification algorithms for recognition of Alzheimer's disease in electrical brain activity (EEG). J Neurosci Methods 161(2):342–350
7. Ahmadlou M, Adeli H, Adeli A (2011) Fractality and a wavelet-chaos-methodology for EEG-based diagnosis of alzheimer disease. Alzheimer Dis Assoc Disord 25(1):85–92
8. Kulkarni N, Bairagi V (2018) EEG-based diagnosis of alzheimer disease: a review and novel approaches for feature extraction and classification techniques. Academic Press, Cambridge
9. Oh SL, Hagiwara Y, Raghavendra U et al (2018) A deep learning approach for Parkinson's disease diagnosis from EEG signals. Neural Comput Appl. https://doi.org/10.1007/s00521-018-3689-5
10. Acharya UR, Oh SL, Hagiwara Y et al (2018) Automated EEG-based screening of depression using deep convolutional neural network. Comput Methods Programs Biomed 161:103–113
11. Acharya UR, Bhat S, Faust O et al (2015) Nonlinear dynamics measures for automated EEG-based sleep stage detection. Eur Neurol 74(5–6):268–287
12. Jasper HH, Proctor LD, Knighton RS, Noshay WC, Costello RT (1958) Reticular formation of the brain. Little, Brown & Company, Boston
13. Chatrian GE, Lettich E, Nelson PL (1985) Ten percent electrode system for topographic studies of spontaneous and evoked EEG activity. Am J EEG Technol. https://doi.org/10.1080/00029238.1985.11080163
14. Medithe JWC, Nelakuditi UR (2016) Study of normal and abnormal EEG. In: 2016 3rd International conference on advanced computing and communication systems (ICACCS), vol 1. IEEE, pp. 1–4
15. Phillips N (2016) Epilepsy with generalized seizures: symptoms, causes, and treatments. Available: https://www.healthline.com/health/generalized-seizures
16. Acharya UR, Hagiwara Y, Deshpande SN, Suren S, Koh JEW, Oh SL, Arunkumar N, Ciaccio EJ, Lim CM (2018) Characterization of focal EEG signals: a review. Future Gener Comput Syst. https://doi.org/10.1016/j.future.2018.08.044
17. Boggs JG (2009) Generalized EEG waveform abnormalities. Retrieved April 25, 2010, from http://emedicine.medscape.com/article/1140075-overview
18. Bhattacharyya A, Pachori RB (2017) A multivariate approach for patient-specific EEG seizure detection using empirical wavelet transform. IEEE Trans Biomed Eng 64(9):2003–2015
19. Hassan AR, Subasi A (2016) Automatic identification of epileptic seizures from EEG signals using linear programming boosting. Comput Methods Programs Biomed. https://doi.org/10.1016/j.cmpb.2016.08.013
20. Zandi AS, Tafreshi R, Javidan M, Dumont GA (2013) Predicting epileptic seizures in scalp EEG based on a variational bayesian gaussian mixture model of zero-crossing intervals. IEEE Trans Biomed Eng 60(5):1401–1413
21. Aarabi A, He B (2017) Seizure prediction in patients with focal hippocampal epilepsy. Clin Neurophysiol 128(7):1299–1307
22. Truong ND, Nguyen AD, Kuhlmann L et al (2018) Convolutional neural networks for seizure prediction using intracranial and scalp electroencephalogram. Neural Netw 105:104–111
23. Alotaiby TN, Alshebeili SA, Alotaibi FM, Alrshoud SR (2017) Epileptic seizure prediction using CSP and LDA for scalp EEG signals. Comput Intell Neurosci. https://doi.org/10.1155/2017/1240323
24. Parvez MZ, Paul M (2017) Seizure prediction using undulated global and local features. IEEE Trans Biomed Eng 64(1):208–217
25. Faust O, Hagiwara Y, Hong TJ et al (2018) Deep learning for healthcare applications based on physiological signals: a review. Comput Methods Programs Biomed. https://doi.org/10.1016/j.cmpb.2018.04.005
26. Acharya UR, Hagiwara Y, Adeli H (2018) Automated seizure prediction. Epilepsy Behav 88:251–261
27. Acharya UR, Sree SV, Alvin AP et al (2012) Application of non-linear and wavelet based features for the automated identification of epileptic EEG signals. Int J Neural Syst 22(02):1250002
28. Tzimourta KD, Tzallas AT, Giannakeas N, et al (2018) Epileptic seizures classification based on long-term EEG signal wavelet analysis. In: IFMBE proceedings
29. Adeli H, Zhou Z, Dadmehr N (2003) Analysis of EEG records in an epileptic patient using wavelet transform. J Neurosci Methods. https://doi.org/10.1016/s0165-0270(02)00340-0
30. Yuan Q, Zhou W, Xu F et al (2018) Epileptic EEG identification via LBP operators on wavelet coefficients. Int J Neural Syst. https://doi.org/10.1142/s0129065718500107
31. Oweis RJ, Abdulhay EW (2011) Seizure classification in EEG signals utilizing Hilbert–Huang transform. Biomed Eng Online 10(1):38. https://doi.org/10.1186/1475-925X-10-38
32. Acharya UR, Sree SV, Suri JS (2011) Automatic detection of epileptic eeg signals using higher order cumulant features. Int J Neural Syst 21(5):403–414
33. Acharya UR, Yanti R, Zheng JW et al (2013) Automated diagnosis of epilepsy using cwt, hos and texture parameters. Int J Neural Syst 23(03):1350009
34. Acharya UR, Vinitha Sree S, Alvin APC, Suri JS (2012) Use of principal component analysis for automatic classification of epileptic EEG activities in wavelet framework. Expert Syst Appl 10:9072–9078
35. George ST, Balakrishnan R, Johnson JS, Jayakumar J (2017) Application and evaluation of independent component analysis methods to generalized seizure disorder activities exhibited in the brain. Clin EEG Neurosci. https://doi.org/10.1177/1550059416677915
36. Subasi A, Gursoy MI (2010) EEG signal classification using PCA, ICA, LDA and support vector machines. Expert Syst Appl 37(12):8659–8666
37. Alotaiby TN, Alshebeili SA, Alshawi T et al (2014) EEG seizure detection and prediction algorithms: a survey. EURASIP J Adv Signal Process 2014(1):183
38. Najafabadi MM, Villanustre F, Khoshgoftaar TM et al (2015) Deep learning applications and challenges in big data analytics. J Big Data 2(1):1
39. Lecun Y, Bengio Y, Hinton G (2015) Deep learning. Nature 521:436–444
40. Coşkun M, Yildirim Ö, Uçar A, Demir Y (2017) An overview of popular deep learning methods. Eur J Tech 7(2):165–176
41. Krizhevsky A, Sutskever I, Hinton GE (2012) ImageNet classification with deep convolutional neural networks. Adv Neural Inf Process Syst. https://doi.org/10.1016/j.protcy.2014.09.007
42. LeCun Y, Boser B, Denker JS et al (1989) Backpropagation applied to handwritten zip code recognition. Neural Comput. https://doi.org/10.1162/neco.1989.1.4.541
43. Uçar A, Demir Y, Güzeliş C (2017) Object recognition and detection with deep learning for autonomous driving applications. Simulation 93(9):759–769
44. Beşer F, Kizrak MA, Bolat B, Yildirim T (2018) Recognition of sign language using capsule networks. In: 2018 26th IEEE signal processing and communications applications conference (SIU)
45. Sarikaya R, Hinton GE, Deoras A (2014) Application of deep belief networks for natural language understanding. IEEE/ACM Trans Audio Speech Lang Process. https://doi.org/10.1109/taslp.2014.2303296
46. Abdel-hamid O, Deng L, Yu D (2013) Exploring convolutional neural network structures and optimization techniques for speech recognition. In: 14th Annual conference of the international

speech communication association (INTERSPEECH 2013), pp 3366–3370
47. Mnih V, Kavukcuoglu K, Silver D et al (2015) Playing atari with deep reinforcement learning Volodymyr. Nature. https://doi.org/10.1038/nature14236
48. Yildirim O, Tan RS, Acharya UR (2018) An efficient compression of ECG signals using deep convolutional autoencoders. Cogn Syst Res. https://doi.org/10.1016/j.cogsys.2018.07.004
49. Yildirim Ö (2018) A novel wavelet sequence based on deep bidirectional LSTM network model for ECG signal classification. Comput Biol Med 96:189–202
50. Acharya UR, Oh SL, Hagiwara Y et al (2017) A deep convolutional neural network model to classify heartbeats. Comput Biol Med. https://doi.org/10.1016/j.compbiomed.2017.08.022
51. Yıldırım Ö, Pławiak P, Tan RS, Acharya UR (2018) Arrhythmia detection using deep convolutional neural network with long duration ECG signals. Comput Biol Med. https://doi.org/10.1016/j.compbiomed.2018.09.009
52. Obeid I, Picone J (2016) The temple university hospital EEG data corpus. Front Neurosci. https://doi.org/10.3389/fnins.2016.00196
53. Srivastava N, Hinton G, Krizhevsky A et al (2014) Dropout: a simple way to prevent neural networks from overfitting. J Mach Learn Res. https://doi.org/10.1214/12-aos1000
54. Lopez S, Suarez G, Jungreis D et al (2016) Automated identification of abnormal adult EEGs. In: 2015 IEEE signal processing in medicine and biology symposium—proceedings
55. American Clinical Neurophysiology Society (2006) Guideline 6: a proposal for standard montages to be used in clinical EEG. J Clin Neurophysiol 23(2):111
56. Chollet F (2015) Keras: Deep learning library for theano and tensorflow. https://keras.io/, 7(8)
57. Lopez S (2017) Automated identification of abnormal EEGs. MS thesis, Temple University. Available: http://www.isip.piconepress.com/publications/ms_theses/2017/abnormal

Terms and Conditions

Springer Nature journal content, brought to you courtesy of Springer Nature Customer Service Center GmbH (“Springer Nature”).
Springer Nature supports a reasonable amount of sharing of research papers by authors, subscribers and authorised users (“Users”), for small-scale personal, non-commercial use provided that all copyright, trade and service marks and other proprietary notices are maintained. By accessing, sharing, receiving or otherwise using the Springer Nature journal content you agree to these terms of use (“Terms”). For these purposes, Springer Nature considers academic use (by researchers and students) to be non-commercial.
These Terms are supplementary and will apply in addition to any applicable website terms and conditions, a relevant site licence or a personal subscription. These Terms will prevail over any conflict or ambiguity with regards to the relevant terms, a site licence or a personal subscription (to the extent of the conflict or ambiguity only). For Creative Commons-licensed articles, the terms of the Creative Commons license used will apply.
We collect and use personal data to provide access to the Springer Nature journal content. We may also use these personal data internally within ResearchGate and Springer Nature and as agreed share it, in an anonymised way, for purposes of tracking, analysis and reporting. We will not otherwise disclose your personal data outside the ResearchGate or the Springer Nature group of companies unless we have your permission as detailed in the Privacy Policy.
While Users may use the Springer Nature journal content for small scale, personal non-commercial use, it is important to note that Users may not:

1. use such content for the purpose of providing other users with access on a regular or large scale basis or as a means to circumvent access control;
2. use such content where to do so would be considered a criminal or statutory offence in any jurisdiction, or gives rise to civil liability, or is otherwise unlawful;
3. falsely or misleadingly imply or suggest endorsement, approval , sponsorship, or association unless explicitly agreed to by Springer Nature in writing;
4. use bots or other automated methods to access the content or redirect messages
5. override any security feature or exclusionary protocol; or
6. share the content in order to create substitute for Springer Nature products or services or a systematic database of Springer Nature journal content.

In line with the restriction against commercial use, Springer Nature does not permit the creation of a product or service that creates revenue, royalties, rent or income from our content or its inclusion as part of a paid for service or for other commercial gain. Springer Nature journal content cannot be used for inter-library loans and librarians may not upload Springer Nature journal content on a large scale into their, or any other, institutional repository.
These terms of use are reviewed regularly and may be amended at any time. Springer Nature is not obligated to publish any information or content on this website and may remove it or features or functionality at our sole discretion, at any time with or without notice. Springer Nature may revoke this licence to you at any time and remove access to any copies of the Springer Nature journal content which have been saved.
To the fullest extent permitted by law, Springer Nature makes no warranties, representations or guarantees to Users, either express or implied with respect to the Springer nature journal content and all parties disclaim and waive any implied warranties or warranties imposed by law, including merchantability or fitness for any particular purpose.
Please note that these rights do not automatically extend to content, data or other material published by Springer Nature that may be licensed from third parties.
If you would like to use or distribute our Springer Nature journal content to a wider audience or on a regular basis or in any other manner not expressly permitted by these Terms, please contact Springer Nature at

onlineservice@springernature.com